**Link to publisher's version:** http://dx.doi.org/10.1061/(ASCE)MT.1943-5533.0001758

# Analysis of strip footings on fibre reinforced slopes with the aid of Particle Image Velocimetry (PIV)

Mehdi Mirzababaei; PhD, Lecturer; Central Queensland University, Melbourne Campus, Victoria, Australia

Mostafa Mohamed*; PhD, Senior Lecturer, Faculty of Engineering and Informatics, University of Bradford, UK

Mohsen Miraftab, PhD, Professor, Institute for Materials Research and Innovation, University of Bolton, UK

*Corresponding author (Email: m.h.a.mohamed@bradford.ac.uk)

**ABSTRACT**

This paper provides results of a comprehensive investigation into the use of waste carpet fibres for reinforcement of clay soil slopes. The interaction between laboratory scale model slopes made of fibre reinforced clay soil and surface strip footing load was examined. Results for the influence of two variables namely fibre content and distance between the footing edge and the crest of the slope are presented and discussed. Particle Image Velocimetry (PIV) technique was employed to study the deformation of the slope under the surface loading. The front side of the tank was made of a thick Perspex glass to facilitate taking accurate images during the loading stage. To study the stress induced in the slope under footing pressure, excess pore-water pressure and total stress increase were measured at predetermined locations within the slope. The results showed that fibre reinforcement increased the bearing resistance of the model slope significantly. For instance, inclusion of 5% waste carpet fibre increased the bearing pressure by 145% at 10% settlement ratio.

## Introduction

Recently, fibre reinforced soils have been examined as a viable engineering material that could mitigate potential collapses of e.g. slopes and embankments. Polypropylene geo-fibres were used in a field trial to repair frequent failure of roadway slope in Beaumont, Texas, USA (Gregory and Chill, 1998). It was reported that the performance of the fibre reinforced slope was enhanced after the addition of fibres. In addition, Ekinci and Ferreira (2012) reported successful application of polypropylene fibres for reinforcing a partially failed embankment located along the M25, London in the UK. Fibres mobilise the tensile resistance of the host soil by interlocking soil particles and forming a composite material with a relatively coherent matrix (see for example; Jamellodin et al., 2010). However, due to the scale of the field projects and associated cost, systematic evaluation of the key parameters affecting the behaviour of fibre reinforced slopes and embankments have not been performed under controlled conditions.

Studies on the use of natural and synthetic fibres such as wool, coir, jute, steel, nylon, polypropylene, polyester, and glass as tension resisting elements have been conducted in the last few decades. Quantification of potential effects of fibres on improving the mechanical response of the reinforced soils under loading was the subject of research (see for example, Santoni and Webster 2001). Several experimentally based studies were undertaken to examine the influence of the key parameters including percentage of fibres, aspect ratio, stress level and testing conditions on the overall behaviour of fibre reinforced granular materials (e.g. Consoli et al., 1998 and 2003; Yetimoglu et al., 2005; Heineck et al., 2005; Diambra et al., 2007; Chen and Loehr, 2008; Hamidi and Hooresfand, 2013; Pino and Baudet, 2015 and Botero et al., 2015). Taking the general consensus of their findings, it is confirmed that addition of small percentage of fibres improves the stress-strain behaviour of fibre reinforced granular soils, unconfined compression strength and ductility and reduces post-peak strength loss. Consoli et al. (2009) observed significant increase in the load carrying capacity of the fibre reinforced sand layers compacted to different relative densities and subjected to plate load test. The maximum improvement was observed when the fibre reinforced sand was compacted to a relative density of 90%. Furthermore, high degree of improvement in the load carrying capacity was recorded at very small strain. These results were in agreement with those of Kumar and Kaur (2012) who reported significant improvement in the ultimate bearing capacity of a poorly graded sand bed reinforced with randomly distributed fibres under plate load test. In a recent study, Nasr (2014) investigated the effects of reinforcing the active zone behind a model sheet pile wall using polypropylene fiber and cement kiln dust. Results attained experimentally and numerically confirmed an increase in the ultimate bearing capacity and ductility of the cemented sand. Bhardwaj and Mandal (2008) undertook centrifuge tests on fibre reinforced fly ash slopes with different gravity ratios and concluded that there is an observable increase in the bearing capacity at failure.

Despite the fact that the mechanical behaviour of cohesive soils is complex, addition of fibres to cohesive soils was found to suppress excessive volume change and brittleness of the compacted cohesive soil at failure (see for example; Maher and Ho, 1994; Kumar et al., 2006; Estabragh et al., 201 and Correia et al., 2015). Moreover, due to the physical interaction between fibres and the cohesive soil particles, higher unconfined compressive strength and flexural strength, increased tensile strength and improved ductility can be achieved (Puppala and Musenda, 2000 and Tang et al., 2007 and Tang et al., 2016). The results of Tang et al., (2007) illustrated that fibre-soil interaction dominantly controlled by the bonding strength and frictional resistance between fibre and soil particles. Fibre reinforcement was also found effective in reducing the number and extent of tension/desiccation cracks, supressing the swelling pressure and increasing the hydraulic conductivity of low permeable clay soils (Al-Akhras et al., 2008, Viswanadham et al., 2009 and Tang et al., 2012).

Most of the studies investigated the addition of virgin fibres with regular length and thickness in a random fashion. However, re-use and recycling of waste fibres is receiving an increasing attention in the UK and worldwide. For example, sustainable approaches for utilisation of carpet waste fibres are highly favourable and are needed to avoid landfilling of 500,000 tonnes/annum in the UK (Mirzababaei, 2013b). The pre- and post-consumer carpet waste fibres are highly variable in length and thickness of individual fibres. A few investigations into reinforcement of soils using waste recycled carpet fibres were reported (Murray et al., 2000, Ghiassian et al., 2004, Fatahi et al., 2012, 2013a,b and Mirzababaei et al., 2013a,b). It was found that similar enhancements to the peak and residual strength of fibre reinforced soils could be achieved by the addition of waste carpet fibres. Murray et al., (2000) suggested that adding 3% of waste carpet fibre was feasible whereas virgin fibres was used with a maximum of 1% from their laboratory tests on sandy silt soils. Based on a series of drained triaxial tests on sand samples reinforced with carpet waste strips, Ghiassian et al., (2004) reported good degree of improvement with either increasing strip content at constant aspect ratio or increasing aspect ratio at constant strip content. Recent studies of Fatahi et al., (2012, 2013a) on application of virgin and carpet fibres showed that improved mechanical behaviour of cement stabilised soft kaolinite can be achieved irrespective of the fibre type. The results of their study showed that although both carpet fibre inclusion and cement addition are effective in shrinkage reduction of clay soils, kaolinite and bentonite clay soils show markedly distinctive behaviour. Carpet fibres were found to be more appropriate for reinforcement of bentonite clay soils whereas cement was quite effective in kaolinite clay soil. In another study Fatahi (2013b) concluded that carpet fibres reduce the shear wave velocity of the cement treated clay soil specimens. However, polypropylene virgin fibres tend to increase the shear wave velocity.

Although, majority of studies were performed in standard testing apparatus, studies on the behaviour of footings constructed on or adjacent to fibre reinforced soil slopes are limited to no single study using waste fibres. This paper therefore aims to explore feasibility and efficiency of waste carpet fibre to enhance the stability of both footing and reinforced soil slope. A series of laboratory scaled model soil slopes reinforced with waste carpet fibres were performed under surface strip footing load. The laboratory tests focused on the effects of; i. fibre content, and ii. distance between footing edge and the crest of the slope. Results for bearing pressure-settlement relation, development of pore water pressure and deformation of fibre reinforced slopes are presented and discussed. The deformation behaviour of the model slopes is estimated using the Particle Image Velocimetry (PIV) technique.

## Materials

Waste carpet fibres supplied by Carpet Recycling UK (www.carpetrecyclinguk.com) as by product waste (i.e., from edge trimming). Table 1 presents the composition and general properties of fibres. The average water absorption of fibres is estimated to be around 1.35% based on the manufacturer's data. The length of fibres ranged from 2 mm to 20 mm with diverse thicknesses from 80 μm to 1500 μm. It is clear that the proposed edge trimming waste carpet fibres have a wide range of aspect ratio. Previous studies pointed out that increasing the aspect ratio leads to higher fibre reinforcement effect (see, Diambra and Ibriam, 2015) and for the same aspect ratio, the fibre reinforcement effect increases with reducing the particle size (see for example, Gray and Al-Refeai, 1986). It should be noted that the aim of the paper is to study the use of waste carpet fibre in stabilising weak soils.

The selection of fibre type and content follows from previous studies by Mirzababaei et al., (2013a,b) in which several investigations were undertaken by the authors examining the workability and efficiency of utilisation of carpet waste fibre on enhancing the behaviour and strength of soils. It was found that mixing of fibres with cohesive soils becomes challenging if more than 5% of waste fibres is added. Nylon carpet waste fibres was mixed successfully with substandard soil up to a maximum of 10 % (Miraftab and Lickfold, 2008). Therefore, a decision was taken to maintain carpet fibres contents of 1%, 3% and 5% so as to relate the outcomes of previous research with the current study.

The soil used in this study is sandy clay with liquid limit of 21.1% and plasticity index of 10.7%. The effective shear strength parameters (cohesion intercept and internal friction angle) of the host soil were determined from consolidated undrained triaxial testing and found to be 5.3 kPa and 32° respectively. A series of standard Proctor compaction tests were carried out on control soil and soil samples mixed with predetermined amounts of fibres of 1 %, 3% and 5%. Fig.1 shows standard Proctor compaction curves for control and fibre reinforced soils. The results show that continuous reduction in maximum dry unit weight and slight increase in optimum moisture content was observed with further increase in fibre content. This is attributed to replacement of soil grains with fibres, which have less specific gravity compared to that of soil grains, and lubricating effect of absorbed water by fibres, which lessens the compaction effort. Similar results have been reported by Kumar et al., (2006) and Harianto et al., (2008). However, to enable meaningful and fair comparison between proposed tests, fibre reinforced slopes need to be constructed to the same dry unit weight and moisture content. Compaction curves indicated that the maximum dry unit weight of the soil with 5% fibre content is the lowest at 17.8 kN/m$^3$. This dry unit weight was then set as practically achievable target in all tests. Based on data presented in Fig. 1, the corresponding water content values for soils with different quantities of fibres compacted to a dry unit weight of 17.8 kN/m$^3$ would be in the range of 16.5~17.5%. It also illustrates that at a moisture content of 16.5%, there is a slight variation on dry unit weight as a function of fibre content. As a result of which, compacting fibre reinforced soils with a water content of 16.5% would result in achieving a dry unit weight of 17.8 kN/m$^3$ ±3%. A series of falling head permeability tests were conducted on samples of unreinforced and fibre reinforced clay soil that were prepared at a dry unit weight of 17.8 kN/m$^3$. The attained results for the coefficient of permeability are shown in Table 2. The results clearly show that fibre inclusion significantly increases the permeability of the clay soil. The permeability coefficient for soil sample with 5% fibre content is over fourfold that recorded for the control soil sample. In the fibre reinforced soil, provided fibres are mixed evenly within the soil, they serve as multi directional pathways for water to drain quicker, thus increasing the coefficient of permeability. The observed behaviour is in agreement with the results reported by Maher and Ho (1994) and Miller and Rifai (2004), who reported increase in hydraulic conductivity of fibre reinforced soils with fibre contents beyond 1%. Coarse sand with $D_{50}$ of 63μm is used at the base of the slope. The sand was compacted to dry unit weight of 18.0 kN/m$^3$ at moisture content of 7%. The coefficient permeability of coarse sand was determined from Constant head permeability test and found to be 4.79 x 10$^{-4}$ m/s.

## Testing Setup

An automated loading machine that is controlled using a Human Machine Interface (HMI) is used to study the behaviour of fibre reinforced slopes. A rigid tank with length of 800 mm, height of 500 mm and width of 300 mm was designed and manufactured to facilitate this study. Fig. 2 shows the laboratory setup. The front side of the tank was made of 15 mm thick Perspex glass to enable observation of the failure mechanism and deformation of the slope under surface loading. Based on the datasheet supplied by the manufacturer, the flexural stiffness of the Perspex glass was found to be 774 $N.m^2$ which might indicate slight deformation under high pressure if care is not undertaken. The tank was therefore braced by a wooden frame all around to minimise/eliminate deformation of the Perspex glass sheet. The back side of the tank was designed so that it provides a number of ports at predetermined locations for the insertion of pressure transducers. The internal sides of the tank were covered with a thin plastic sheet so as to eliminate wall friction effects.

A solid steel rigid model footing with a width of 50 mm and length of 297 mm was used to simulate plane strain conditions. Load was applied in the centre of the footing through a ball bearing mechanism. The footing was driven axially downwards at the rate of 1 mm/min until a settlement value of 12.5 mm was recorded and the corresponding axial load was measured using a 5 kN load cell. Settlement of the footing was accurately measured using two LVDT mounted on both sides of the loading point. Measurements of load and settlement were recorded every 20 s. To measure the induced excess pore-water pressure, two pressure transducers with ceramic disc of 500 kPa air entry value were inserted into the back of the slope at predetermined locations. The surface of pressure transducers' ceramic discs was smeared with a saturated kaolinite paste to improve the interface between the pressure transducer's ceramic disc and the compacted clay soil. Pressure transducers were saturated for 72 hours prior to testing using a developed saturating cylinder to apply cycles of -90 kPa (with the aid of a vacuum pump) and +1800 kPa (using a GDS pressure controller). Pressure transducers were calibrated prior to use and their accuracy was found to be within ±1 kPa. Three mini load cells with capacity of 700kPa and accuracy of ±0.7 kPa were also utilised for measurements of the total stress at the base of the slope. Measurements from the pressure transducers and load cells were recorded electronically through data acquisition system every 1 s.

## Experimental programme and procedure

Fig. 3 shows a schematic drawing for the geometry of the model slope, locations of the strip footing, load cells and pressure transducers in each series of tests. A total of 11 experiments in 3 series were conducted to examine the behaviour of unreinforced and fibre reinforced soil slopes with 1%, 3% and 5% fibre content. In this paper, Footing Edge Distance Ratio (FEDR) is introduced as a dimensionless ratio of the distance between nearest edge of the footing and crest of the slope (see, distance X in Fig. 3) over the width of the footing. Three different FEDRs of 0, 1 and 3 were studied for both unreinforced and fibre reinforced model slopes. All model slopes were constructed with a slope angle of 45° overlying a layer of 100 mm thick compacted sand layer so as to provide a relatively stiff permeable boundary for the slope and to enhance capturing the stress change at the base.

One of the challenges encountered in this study is how to ensure preparation of a homogenous fibre reinforced soil in large quantity. Up-to-date, there is a lack of standardised mixing procedure for preparation of homogeneous fibre reinforced soils (Botero et al., 2015). Moist tamping and moist vibration techniques have been found effective in preparation of homogeneous granular soil samples for experimental studies but they are not fairly satisfying to produce isotropic distribution of fibres (Ibraim et al., 2012). Diambra et al., (2007) showed that preparing coarse grained fibre reinforced soil samples by moist tamping technique results in 97% of the fibres are oriented preferentially at ±45° to the horizontal axis. Results of Saad et al., (2012) demonstrated that increasing the number of soil layers and compressing the soil sample from both ends results in even distribution of fibre within the specimen, and improves the uniformity of density profile and the integrity of fibre reinforced samples. It was reported that the proposed static approach enhance the repeatability of the unconfined compression strength test results. On the other hand, Diambra and Ibraim (2014) claimed that in fibre reinforced kaolinite clay samples consolidated from slurry, the orientation of fibres is rather isotropic. Despite the fact that preparation of homogenous randomly oriented fibre reinforced soils is challenging, most of the problems could be minimised or eliminated by decreasing the amount of added fibres and increasing the water content of fibre reinforced cohesive soils (Mirzababaei et al. 2013b).

In this paper to produce a relatively homogenous mix, a rotary drum mixer was used. Dry soil and fibres were mixed initially followed by adding predetermined amounts of water upto reaching the desired moisture content. The mixing process was then continued until a uniform mixture was achieved. The geometry of the slope was marked on back wall of the tank and the model slope was subsequently constructed in five equal compacted layers of 50 mm thick by tamping technique. Before placing the following layer, the surface was scratched with a spatula and the procedure was continued until reaching the full height of slope. Once the slope was constructed, it was covered by polyethylene sheet to prevent evaporation of water from the soil slope. The slope was then left for a period of 24 hours which was found sufficient to reach equalisation of water within the slope. Samples have been extracted from different locations within the slope to examine the uniformity of density and fibre distribution. It was found that density varies within a range of ±7.3 % and fibre content is within ±17%. This highlights that further work is needed to further enhance the uniformity of fibre and density. The model footing was placed on the surface at the required FEDR. The model footing was then loaded in such way so that a settlement rate of 1 mm/min was attained in all tests.

## PIV Technique

Particle Image Velocimetry (PIV) theory was first introduced by Adrian (1991) in the field of fluid mechanics. The technique relies on taking images of a seeded surface and tracking the movement of individual particles in consecutive images. PIV method has slightly been modified to fit Geotechnical Engineering testing. PIV is advantageous over other techniques since deformation of the soil can be determined non-invasively without causing any disturbance to the testing process. Application of PIV method in naturally textured soils such as sand with different coloured grains does not require any extra process to create pseudo-texture. However, to create a suitable contrast that is recognisable when illuminated, it is required to introduce texture to the surface of the clay soil by addition of dyed particles such as coloured sand (White et al., 2003). In this study, the front side of slope was sprayed with coloured sand so as to enhance the visibility of the slope and its deformation.

Dynamic Studio package (www.DantecDynamics.com) was used to perform PIV analysis on the acquired images. All images in this study were taken using a Nikon D90 camera with a resolution of 12M Pixel. The camera was positioned 1.0 m away with its optical axis at right angle to the front surface of the tank. The size of the view field was 387.4 mm x 257.3 mm. Given, the size of the images (4288x2848 pixels), the scale of the view field was determined to be 0.090345 mm/pixel. To verify the accuracy of the deformation results from PIV analysis, an arbitrary point A was selected at a distance of 50 mm from the centre of the footing at the top surface of the slope (see, Fig. 4). The displacement of Point A was then determined against a stationary point on the tank in two photographs that were taken before loading and at footing pressure of 50 kPa using scaling method in AutoCAD. The results of the vertical displacement of Point A is 0.3 mm whereas that given by PIV analysis is 0.29674 mm (see, Fig. 6). Therefore, the accuracy of the PIV technique in this study was considered to be acceptable.

## Results and Discussion

Data for the footing pressure and settlement, deformation of the slope, induced excess pore-water pressure and the total stress increase at the base of the slope are generated and discussed in this section to highlight the impact of studied parameters on the behaviour of fibre-reinforced clay slopes. It should be noted that a non-dimensional Footing Settlement Ratio (S/B) is utilised hereafter where; S stands for the footing settlement and B denotes the footing width. The following sections are organised to discuss the effects of fibre reinforced slopes that were loaded at three different FEDRs on:

a) Relationship between footing pressure and settlement ratio;
b) Contours of horizontal and vertical displacements of the slope at a footing pressure of 50 kPa; and
c) Excess pore-water pressure and total stress increase.

Of note, a bearing pressure of 50 kPa for analysis of the results was selected as it was found to be the maximum footing pressure of the unreinforced slope. Since, images and footing pressure measurements were taken every 20 s, it was straightforward exercise to select the image corresponding to or very close to the required pressure for PIV analysis.

## Footing Edge Distance Ratio of three

Fig. 5 shows the results of the relationships between the footing pressure and settlement ratio for fibre reinforced slopes with fibre content of 0, 1%, 3% and 5%. In this series, all tests were performed on the footing placed at FEDR of 3. The results clearly demonstrate that addition of fibres enhances the stiffness of the fibre reinforced slopes. The figure confirms the significant increase in the ultimate bearing capacity with increasing fibre content. Fibre reinforced slopes with 3% and 5% fibre contents showed 85% and 145% increase in the measured footing pressure at 10 % settlement ratio respectively over that attained for unreinforced slope. The increase in footing bearing pressure can be attributed to the reinforcement effects as a result of enhanced interlocking, higher shear strength parameters of reinforced soils and higher passive resistance. The figure also suggests that as the percentage of fibre increases the failure mode changes from punching shear failure on slope with 0% fibre content to a general shear failure over large area at 5% fibre content. The relationship between the footing pressure and settlement ratio of the 5% fibre reinforced model slopes is found to be almost linear for the range of footing-settlement ratio between 3% and 25% indicating elastic behaviour of the fibre reinforced material. Careful inspection of Fig. 5 illustrates that for the same footing pressure, less settlement/movement is experienced with increasing fibre content. This is due to increased stiffness of fibre compacted soils (Mirzababaei et al., 2013a) and increased number of fibre per unit volume and the corresponding interfacial area (Tang et al., 2016). This is also in good agreement with previous results published by Estabragh et al., (2011) on a series of undrained triaxial tests on reinforced soft clay soils with nylon fibres.

Horizontal and vertical displacement contours obtained using PIV technique of unreinforced and 5% fibre reinforced slopes at footing pressure of 50 kPa are presented in Fig. 6a-d respectively. Of note, horizontal displacement towards the right and upward vertical displacement are considered to be positive. Results presented in Fig. 6a for the unreinforced clay slope show a typical deformation pattern of unreinforced soil slope in which a tendency to deform laterally towards the free slope surface is high and very little deformation is recorded for soil particles underneath the centre of the footing. Significant lateral deformation is noticeable down to a depth of 2B. Comparing data presented in Figs. 6a and b illustrates that the lateral deformation of 5% fibre reinforced slope is markedly smaller than that experienced for the unreinforced slope for the same soil depth. This could be attributed to the high degree of interlocking and improved shear strength parameters. As a result, the reinforcing fibres transfer developed shear stresses beneath the loaded area to adjacent stable soil zones resulting in a wider and deeper failure. Furthermore, existence of fibres within the soil skeleton reduces the movement of soil particles due to their pull out resistance which is controlled by the interfacial shear resistance at the fibre-soil interface. Therefore, the reinforced soil not only result in increasing the bearing resistance due to developing larger failure zone but also reduce the stress level underneath the loaded area leading to reduced deformation.

Analysis of the vertical displacement contours in Fig. 6c for unreinforced soil slope illustrates that settlement of the slope extends laterally to a region of ± B from the centre of the footing beyond which the soil heaves in both sides. The results also indicated that significant deformation occurred underneath the footing taking the shape of a bulb and extending down to a depth of 2B. However, the vertical deformation pattern of fibre reinforced slope with 5% fibre content is observed to be characteristically different as shown in Fig. 6d. The vertical deformation is significantly lower, decreases with depth and covers larger area of the slope. The soil heaved after a distance of ±2B. This illustrates that fibres integrated relatively well with the soil particles to form a relatively uniform composite material that able to dissipate the energy under the loaded area compared to unreinforced soil. This is in good agreement with the postulation of Jamellodin et al., (2010)'s observation of significant improvement in the failure deviator stress and shear strength parameters of the soft soil reinforced with palm fibres.

Fig. 7 shows the evolution of excess pore-water pressure at predetermined locations as presented in Fig. 3d. It is clear from Fig. 7 that zero excess pore water pressure was recorded at all measurement points before the start of loading. This confirms that leaving the constructed slope for 24 hrs was sufficient to reach stabilisation of water. Data recorded for the excess pore water pressure show that positive excess pore water pressure is recorded in the soil part of the slope that is in the left hand side of the footing irrespective of the settlement ratio. In addition, unreinforced soil slope experienced higher positive excess pore pressure. This is likely due to the confinement of soil in this part of the slope leading to contraction of the soil. In contrast, the excess pore water pressure distribution measured in the right hand side showed a slightly negative values. The observed excess pore-water pressure is related to the deformation pattern and permeability of the unreinforced and reinforced soil slopes at the measurement locations. For unreinforced soils in the right hand side of the footing, the deformation patterns suggest that the soil is under compression leading to high positive excess pressure which is further amplified by the inability of the soil to dissipate excess water pressure due to its low coefficient of permeability. In contrast, the deformation pattern in the part of slope to the right hand side suggests a slight dilative behaviour leading to a small negative pressure measurements that are close to zero. It can be shown that fibre reinforced slope with 5% fibre content resulted in less generated excess pore-water pressure at both sides of the footing. This is due to the higher permeability of the fibre reinforced soil compared to unreinforced soil (see, Table 2) which  speeds dissipation of induced excess pore-water pressure during loading.

## Footing Edge Distance Ratio of one

A second series of tests were performed on soil slopes with 0, 1% and 3% fibre contents at FEDR of 1. Fig. 8 shows the results of load deformation behaviour of unreinforced and fibre reinforced slopes. Substantial enhancement can be observed on fibre reinforced slope with 3% fibre content. At a settlement ratio of 10%, the measured bearing pressure is 61 kPa yielding an increase of about 76% over that measured for unreinforced slope. No significant effect can be observed in the load carrying capacity for a soil slope reinforced with 1% fibres. The results of 3 % fibre is similar to those obtained for FEDR of 3 suggesting that fibre reinforced soil distribute the developed stress well over larger area. The load-deformation behaviour shown in Fig. 8 also confirms the increase in stiffness of the fibre reinforced soil with increase in fibre content.

Figs. 9a-d show horizontal and vertical displacement contour lines under the footing for unreinforced and 3% fibre reinforced slopes. Examining the deformation in the right hand side of footing shows that movement of soil particles is primarily towards the free face of the slope. As it can be seen in Fig. 9a, the lateral deformation of the unreinforced slope is still significant down to the depth of 3B. However, its vertical settlement is limited to a depth of 2B as shown in Fig. 9c. Fig. 9b clearly shows that fibre inclusion has limited the soil lateral deformation of the slope. These results are in harmony with previously report results that fibres reduce movement of soil particles and desiccation cracks due to bonding strength and frictional resistance between fibre and soil particles as suggested (Tang et al., 2007 and Tang et al., 2016). Fig. 9d demonstrates that the vertical settlement of the soil under footing load has been decreased significantly with increase in fibre content. However, the vertical settlement of the slope is not uniform compared to the deformation pattern of FEDR of 3 with

5% fibre content (Fig. 6d). Fig. 10 shows the excess pore-water pressure behaviour for model slopes with unreinforced and 3% fibre reinforced slope measured under the footing's centre (see Figure 3c). Measurement of excess pore-water pressure below the footing showed higher values for unreinforced soil than reinforced soil. This is mainly due to the higher permeability of the reinforced soil leading to swift drainage of pore water and dissipation of excess pore-water pressure. As previously mentioned the part of the soil slope in the left hand side of the footing is under compression whereas the right hand side of the slopes seems to be undergoing very limited dilative behaviour.

**Footing Edge Distance Ratio of zero**

The load-settlement curves on the model slopes at FEDR of 'Zero' with fibre content of 0%, 1%, 3% and 5% are presented in Fig. 11. Footing pressure curves of fibre reinforced slope with 3% and 5% fibre contents were significantly distinctive from those of unreinforced and 1% fibre content. This figure also shows significant increase in the stiffness of the fibre reinforced soil with increase in fibre content. Increase in fibre content to 3% and 5% resulted in 71% and 97% increase in the footing bearing pressure respectively over that of unreinforced slope at footing settlement ratio of 10%. The relationship between footing pressure and settlement ratio on a soil slope reinforced with 5% fibre content was found to be highly linear over the measured range of settlement ratio up to 25%. Such linear elastic load-deformation behaviour was also seen for the case of 5% fibre reinforced slope with FEDR of 3. This elastic behaviour is attributable to; i. the structure of fibre reinforced soils due to addition of high percentage of fibres which are tangled around soil particles leading to increased shear resistance, and ii. the overburden pressure created by settlement. These results highlight that for a 5% fibre reinforced soil, fibres are still in phase 1 which is pure elastic phase out of the five progressive pull out phases proposed by Zhu et al. (2014). Data for 1% fibre content show no enhancement to the behaviour of fibre reinforced soil slope which is consistent with those recorder at FEDR of 1. Previous studies confirmed that substantial loss in the footing bearing pressure is observed as the footing location becomes closer to the crest. However, utilisation of fibre as reinforcing elements spreads the generated shear stresses underneath the loaded area out over larger area which contributes significantly to increase in the bearing pressure in comparison with that measured for unreinforced soil slope.

Data for the horizontal and vertical displacement contour lines under the footing for unreinforced and 5% fibre reinforced slopes are presented in Figs. 12a-d. It is clear that the horizontal and vertical deformations of unreinforced soil slope are markedly higher than those experienced at lower value of FEDRs. The lateral deformation of the unreinforced slope is noticeable to a depth of 3B. However, its vertical settlement is limited to the depth of 2.5B. Comparing Figs. 6a, 9a and 12a demonstrates that the extent of lateral and vertical deformation within the unreinforced soil has been influenced by the location of the footing with respect to the slope face. With 5% fibre content, the deformation of the reinforced soil slope decreased significantly showing consistently small deformation through the whole body of the slope (Figs. 12b and d). The displacement patterns measured at different FEDRs for unreinforced and fibre reinforced soil slopes indicate that fibres acted by holding the soil particles from moving towards the slope face resulting in reduced horizontal deformation. This leads to spreading the footing pressure deeper and wider area which in turn means a longer failure surface, greater bearing capacity and reduced vertical deformation.

Fig. 13 shows the excess pore-water pressure behaviour of the slope with FEDR of 'zero' at predetermined locations (see, Fig. 3d). Low negative excess pore-water pressure was measured for unreinforced slope in the right side of the footing due to displacement of the soil slope at this location towards the free slope surface (Figs. 12a and c). However, for fibre reinforced slopes, the measured excess pore-water pressure at the same location was almost close to zero due to its higher permeability and less deformation compared to unreinforced slope. The positive excess pore-water pressure measured at left side of the footing for unreinforced model slopes is indicative of compression behaviour of soil in this region. This can be further explained through deformation patterns of the slope with settlement and lateral deformation to the confined side of the tank (Figs. 12a and c). However, with 5% fibre inclusion, the measured excess pore-water pressure is close to 'zero' due to higher permeability of the reinforced soil compared to unreinforced soil.

**Total stress increase at the base**

Measurements for the increase in total stress were taken at three points at the base of the constructed slopes as given in Fig. 3. Fig. 14 presents the measured increase in the total stress at the base of the slopes on slopes tested at different values of FEDRs and fibre contents under a footing pressure of 50 kPa. The data shown in this figure demonstrate that to a great extent the measured stress distribution is typical in which vertical stress is high underneath the centre of the loaded area and decays as measurement point moves away from the centre. Furthermore, with increasing the fibre content in the soil slope transfer of stress is considerably enhanced reaching deeper layers and causing considerable increase in total stress below the centre point of the loaded area. The observed stress behaviour is directly linked to the shear strength of the fibre reinforced soils. Previous studies (see for example

Mirzababaei et al., 2013a and Tang et al., 2007) reported the enhanced shear strength parameters with the increased amount of fibres which in turn result in lowering the horizontal shear stress and enhancing the transfer of vertical stress.

This is in agreement with the observed deformation pattern from PIV analysis that showed a uniform deformation pattern of the fibre reinforced slope over a larger area. This proves that fibres integrated relatively well with the soil particles forming a relatively uniform strengthened composite material that can offer higher resistance to loads. In unreinforced soil slope, the horizontal and vertical displacements are intensified over smaller areas that are close to the loaded area. This would result in substantial movement of soil particles near soil surface due to concentration of stress. The measured increase in total stress at the left side of the footing is slightly less than that of measured at right of the footing. This could be attributed to the movement of soil towards the free face of the slope and wall effects that counteract the stress transfer. In addition, due to the slight variation of density and fibre content across the slope, stress transfer would be influenced.

**Coupled effect of the footing location and fibre content**

To summarise the coupled effect of FEDR and fibre content on the footing bearing pressure, a 3D graph has been plotted and presented in Fig. 15. Of note, all bearing pressure measurements were taken at a settlement ratio of 10%. This figure shows that pronounced effect for fibre addition is clear making it an efficient technique to overcome potential loss in the bearing pressure for footings constructed in close proximity to slope faces. High degree of bearing pressure enhancement is observable irrespective of the footing edge distance ratio in comparison with those attained on unreinforced soil slope. Fig. 16 shows cross sections of the failed area on unreinforced soil and reinforced soil with 5% fibre content. The results indicated clearly that fibres integrated and interlocked well with the soil particles forming a relatively homogenous reinforced soil. There are no visible cracks observed on fibre reinforced soil. Nevertheless, very clear punching shear failure is noticeable on unreinforced soil slope. These suggest that on fibre reinforced soils there is high degree of stress transfer to adjacent and deeper areas that are more stable which in turn leads to wider and deeper failure surface. Hence the footing deformation reduces substantially with the increase in fibre content.

**Scale and boundary effects**

Due to difficulties and associated cost to load full scale model footings under controlled conditions to failure, studies based on experimental models are commonly performed. Although, the whole system is scaled down to a laboratory scale, the use of such models are useful to acquire deeper understanding of the behaviour of slopes and foundations on or close proximity to the slope face (see for example; Choudhary et al., 2010 and Castelli and Lentini, 2012). Careful design of the laboratory scaled models is required to ensure that the observed behaviour can be extrapolated to larger scale. However, it is likely that scale effect might cause some influence on experimentally attained results (Vesic, 1973). Key parameters for consideration in small scale fibre reinforced soil slopes include footing size, particle size distribution, density, fibre aspect ratio, wall friction and boundary conditions.

Recently Toyosawa et al., (2013) stated that there is no effect for the model footing size on the bearing capacity if the ratio of footing diameter to particle size is more than 50. Earlier reporting suggested the ratio of footing width to particle diameter has to be more than 200 to eliminate scale effects (see for example; Habib, 1974). In this study, the ratio of the footing width to the median diameter of the sandy clay material is close to 250 which is satisfactory. Considering the aspect ratio and length of fibre, Diambra and Ibriam (2015) concluded that to achieve the desired effect of fibres, the aspect ratio is required to be between 10 and 100 and fibre length is at least 10 times the average particle size which have been met in the current study. However, controlling the aspect ratio and fibre length of waste is extremely difficult. So, it seems reasonable that further experimentations are needed to increase understanding of fibre reinforced effects with variable fibre aspect ratio and fibre length.

Jayasree et al., (2012) based on numerical simulations suggested that wall effects could be reduced by increasing tank width to footing width ratio and reducing angle of friction between soil and tank sides. In this study, all tests were performed under plain strain conditions in a tank with a length and width of 16 and 6 times the width of footing to reduce wall effects and to provide some flexibility in positioning the footing with respect to the slope face. The tank sides are covered by plastic sheet to minimise wall effects. Centrifugal compression tests on fibre reinforced slopes would be recommended to provide deeper understanding of the real behaviour.

## Conclusions

A comprehensive and systematic laboratory study into the effects of fibre content and footing edge ratio on the behaviour of slope under surface loading was undertaken. Particle image velocimetry technique was employed to investigate the deformation pattern of the slope throughout the experiments. Excess pore-water pressure behaviour and total stress increase at predetermined locations within the slope were also measured using a set of instrumentations. Based on the experimental analysis, the following conclusions can be made:

- Fibre reinforcement enhanced the bearing resistance of the model slopes significantly. The footing pressure on 5% fibre reinforced model slope showed 145% improvement over that attained on unreinforced model slope at footing edge distance ratio of 3.
- The use of fibres increased the strength of the reinforced soil slope due to the interlocking of the soil particles with fibres resulting in a reduced deformation of the slope in both vertical and lateral directions. Moreover, fibres enhanced the integrity of the slope and prevented occurrence of tension cracks at failure. The stiffness of the slope increased significantly with increase in fibre content that resulted in less deformation of fibre reinforced slopes for the same footing pressure.
- In fibre reinforced model slopes, degree of stress transfer is higher which is attributed to enhanced shear strength and confinement.
- In general, addition of 1% Fibres showed insignificant improvement in the footing bearing pressure for all footing edge distance ratios.
- Fibre reinforced slopes with 5% fibre showed high degree of elastic behaviour so that the footing pressure-settlement ratio relationships was almost linear over the range of settlement ratio upto 25%.

## References

Adrian, R.J. (1991). "Particle imaging techniques for experimental fluid mechanics. Annual Review of fluid Mechanics", 23, 261-304.

Al-Akhras, N.M., Attom, M.F., Al-Akhras, K.M., Malkawi, A.I.H. (2008). "Influence of fibres on swelling properties of clayey soil" Geosynthetics International Journal, 15(4), 304-309

Bhardwaj, D.K., Mandal, J.N. (2008). “Centrifuge modelling on fibre reinforced fly ash slope” In: proceedings of the 4th Asian Regional Conference on Geosynthetics, Shanghai, China.

Botero, E., Ossa, A., Sherwell, G., and Ovando-Shelley, E. (2015). “Stress-strain behavior of a silty soil reinforced with polyethylene terephthalate (PET)” Geotextiles and Geomembranes, 43(4), 363-369.

Castelli, F and Lentini, V. (2012). “Evaluation of the bearing capacity of footings on slopes”. Int. J. of Physical Modelling in Geotechnics, 12(3), 112-118.

Chen, C.W. and Loehr, J.E. (2008). “Undrained and drained triaxial tests of fibre-reinforced sand” In: Proceedings of the 4th Asian Regional Conference on Geosynthetics. Shanghai, China, 114-120.

Choudhary, A.K., Jha, J.N. and Gill, K.S.(2010).” Laboratory investigation of bearing capacity behaviour of strip footing on reinforced flyash slope”. Geotext and Geomemb., 28, 393-402.

Consoli, N.C., Casagrande, M.D.T., Thome, A.R., Dalla Rosa, F. and Fahey, M. (2009). “Effect of relative density on plate loading tests on fibre-reinforced sand” Geotechnique, 59(5), 471-476.

Consoli, N.C., Corte, M.B., Festugato, L. (2012). “Key parameter for tensile and compressive strength of fiber-reinforced soil lime mixtures” Geosynth. Int., 19(5), 409-414.

Consoli, NC., Prietto, M., Ulbrich, A. (1998). “Influence of fibre and cement addition on behavior of sandy soil” J. of Geotechical Engineering, 124(12), 1211-1214.

Consoli, N., Casagrande, M., Prietto, P., and Thomé, A. (2003). "Plate Load Test on Fiber-Reinforced Soil." J. Geotech. Geoenviron. Eng., 10.1061/(ASCE)1090-0241(2003)129:10(951), 951-955

Correia, A., Venda Oliveira, P., and Custódio, D. (2015). "Effect of polypropylene fibres on the compressive and tensile strength of a soft soil, artificially stabilised with binders" Geotext. Geomemb., 43(2), 97-106.

Diambra, A. and Ibraim, E. (2015). “Fibre-reinforced sand: interaction at the fibre and grain scale” Geotechnique 65 (4), 296-308.

Diambra, A., Ibraim, E. (2014). “Modelling of fibre-cohesive soil mixtures” Acta Geotechnica, 9, 1029-1043.

Diambra, A., Russell, A.R., Ibraim, E. and Muir Wood, D. (2007). “Determination of fibre orientation distribution in reinforced sands” Geotechnique, 57(7), 623-628.

Ekinci, A. and Ferreira, P.M.V. (2012). “The undrained mechanical behaviour of a fibre-reinforced heavily over-consolidated clay” ISSMGE-TC 211 International Symposium on Ground Improvement, Brusseles.

Estabragh, A., Bordbar, A., Javadi, A. (2011). “Mechanical Behaviour of a Clay Soil Reinforced with Nylon Fibres” J. of Geotechnical and Geological Engineering, 29, 899-908.

Fatahi, B., Fatahi, B., Le, T.M. and Khabbaz, H. (2013b). “Small-strain properties of soft clay treated with fibre and cement” Geosynthetics International, 20(4), 286-300.

Fatahi, B., Khabbaz, H. & Fatahi, B. (2012). “Mechanical characteristics of soft clay treated with fibre and cement” Geosynthetics International J., 19(3), 252-262.

Fatahi, B., Le, T.M., Fatahi, B., Khabbaz, H. (2013a). “Shrinkage Properties of Soft Clay Treated with Cement and Geofibers” Geotechnical and Geological Engineering J., 31, 1421-1435.

Ghiassian, H., Poorebrahim, G. and Gray, D. (2004). “Soil Reinforcement with Recycled Carpet Wastes” Waste Management & Research J., 22(2), 108-114.

Gray, D. H. and Al-Refeai, T. O. (1986). “Behaviour of fabric- versus fiber-reinforced sand” J. Geotech. Engng, ASCE 112(8), 804-820.

Gregory, G.H. and Chill, D.S. (1998). “Stabilization of earth slopes with fibre reinforcement” Proceedings of the sixth International conference on geosynthetics, Atlanta, Georgia, 1073-1078.

Habib, P.A. (1974).” Scale Effect for Shallow Footings on Dense Sand” J. of the Geotech. Eng. Division, ASCE, 100 (1), 95-99.

Hamidi, A., Hooresfand, M. (2013). “Effect of fiber reinforcement on triaxial shear behaviour of cement treated sand”. Geotext. Geomemb., 36, 1-9.

Harianto, T., Hayashi, S., Du, Y.J., Suetsugu, D. (2008). “Effects of Fiber Additives on the Desiccation Crack Behavior of the Compacted Akaboku Soil as A Material for Landfill Cover Barrier” J. of Water Air Soil Pollut., 194(1), 141-148

Heineck, K., Coop, M., and Consoli, N. (2005). "Effect of Microreinforcement of Soils from Very Small to Large Shear Strains" J. of Geotechnical and Geoenvironmental Engineering, 131(8), 1024-1033.

Ibraim, E., Diambra, A., Russell, A.R., Muir Wood, D. (2012). “Assessment of laboratory sample preparation for fibre reinforced sands” Geotext. Geomemb., 34, 69-79.

Jamellodin, Z., Talib, Z., Kolop, R., Noor, N. (2010). “The effect of oil palm fibre on strength behaviour of soil” In: 3rd SANREM conf., kota kinabalu, Malaysia; 3–5 August.

Jayasree, P. K., Rajagopal, K., and Gnanendran, C.T. (2012). “Influence of Sidewall Friction on the Results of Small-Scale Laboratory Model Tests: Numerical Assessment” Int. J. Geomech., 2012, 12(2): 119-126.

Kumar A., Kaur A. (2012). "Model tests of square footing resting on fibre reinforced sand bed" J. of Geosynthetic International, 19(5), 385-392.

Kumar, A., Walia, B.S. and Mohan, J. (2006). "Compressive strength of fibre reinforced highly compressible clay" Construction and Building Materials, 20, 1063-1068.

Maher, M.H. and Ho, Y.C. (1994). "Mechanical properties of kaolinite/fibre soil composite" J. of Geotechnical Engineering, 120(8), 1381-1393.

Miller, C. J. and Rifai, S. (2004). "Fiber reinforcement of waste containment soil Liners" J. of Environmental Engineering, 130(8), 891-895.

Miraftab, M. & Lickfold, A. (2008). "Utilization of carpet waste in reinforcement of substandard soils" Journal of Industrial Textiles, 38(2), 167-174.

Miranda Pino, L. and Baudet, B. (2015). "The effect of the particle size distribution on the mechanics of fibre-reinforced sands under one-dimensional compression". Geotext. Geomemb., 43(3), 250-258.

Mirzababaei, M., Miraftab, M., Mohamed, M. and McMahon, P. (2013a). "Unconfined compression strength of clays with waste carpet fibres" J. of Geotechnical and Geoenvironmental Engineering, 139(3), 483-493.

Mirzababaei, M., Miraftab, M., Mohamed, M. and McMahon, P. (2013b). "Impact of waste carpet fibres on swelling properties of compacted clays" J. of Geotechnical and Geological Engineering, 31(1), 173-182.

Murray, J. J.; Frost, J. D. and Wang, Y. (2000). "Behaviour of a sandy silt reinforced with discontinuous recycled fibre inclusions" Transportation Research Record J., 1714(1), 9-17.

Nasr, A.M. (2014). "Behavior of strip footing on fiber-reinforced cemented sand adjacent to sheet pile wall" Geotext. Geomemb., 42(6), 599-610.

Puppala, A.J., Musenda, C. (2000). “Effects of Fiber Reinforcement on Strength and Volume Change in Expansive Soils” Transportation Research Record J., 1736, 134-40.

Saad, S., Mirzababaei, M., Mohamed, M., Miraftab, M. (2012). “Uniformity of density of compacted fibre reinforced clay soil samples prepared by static compaction”, The 5th European Geosynthetics Congress, Valencia, Spain.

Santoni, R.L., and Webster, S.L. (2001). “Airfields and road construction using fibre stabilization of sands” J. of Transport Engineering, 127(2), 96-104.

Tang, C., Shi, B., Gao, W., Chen, F., and Cai, Y. (2007). “Strength and mechanical behavior of short polypropylene fiber reinforced and cement stabilized clayey soil” Geotext. Geomembr. 25(3), 194-202.

Tang, C., Shi, B., Cui, Y., Liu, C., and Gu, K. (2012). “Desiccation cracking behaviour of polypropylene fibre-reinforced clayey soil. Can. Geotech. J., 49: 1088-1101.

Tang, C., Wang D., Cui, Y., Shi, B., and Li, J. (2016). “Tensile strength of fibre-reinforced soil” J. of Materials in Civil Engineering, ASCE, 8(7), 04016031-13.

Toyosawa, Y., Itoh, K., Kikkawa, N., Yang, J. and Liu, F. (2013).” Influence of model footing diameter and embedded depth on particle size effect in centrifugal bearing capacity tests” Soils and Foundations, 53(2), 349-356.

Vesic, A. (1973).”Analysis of ultimate loads of shallow foundations”. J. of Soil Mechanics and Foundations Division ASCE, 94(SM3), 661-688.

Viswanadham, B.V.S., Phanikumar, B.R. and Mukherjee, R.V. (2009). “Swelling behaviour of a geofibre-reinforced expansive soil” Geotext. Geomemb., 27, 73-76.

White, D. J., Take, W. A. and Bolton, M. D. (2003). “Soil deformation measurement using particle image velocimetry (PIV) and photogrammetry”, Geotechnique, 53(7), 619-631.

Yetimoglu, T., Inanir, M., Inanir, O. (2005). “A Study on Bearing Capacity of Randomly Distributed Fiber-Reinforced Sand Fills Overlying Soft Clay” Geotext. Geomemb., 23 (2), 174-183.

Zhu, H., Zhang, C., Tang, C., Shi, B. and Wang B. (2014) “Modelling the pullout behaviour of short fiber in reinforced soil. Geotext. Geomemb., 42: 329-338.

List of tables

Table 1: Properties of waste carpet fibres

| **Fibre Type** | **Specific Gravity*** | **Water Absorption* (%)** | **Composition (%)** | **Specific Tensile Modulus* ($GPa/gr/cm^3$)** |
|---|---|---|---|---|
| Polypropylene | 0.90 | Nil | 60 | 0.27~0.44 |
| SBR Latex | 0.99 | - | 20 | - |
| Nylon | 1.14 | 4.1-4.5 | 15 | 0.40~0.70 |
| Wool | 1.32 | 13-15 | 5 | 0.27~0.40 |

*Recommended by the manufacturer

Table 2: Permeability coefficients of clay samples with different percentages of fibre

| Fibre content % | Permeability (m/sec) x $10^{-10}$ |
|---|---|
| 0 | 2.27 |
| 1 | 4.15 |
| 3 | 4.99 |
| 5 | 9.92 |

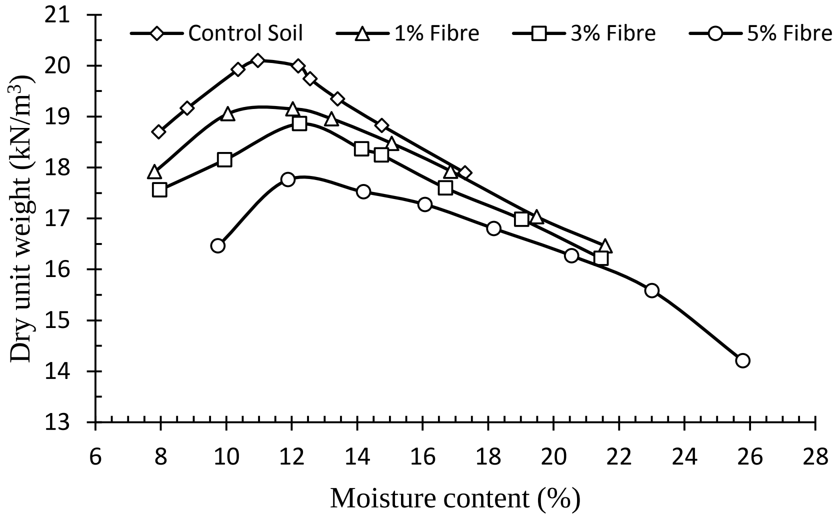


Fig. 1. Standard Proctor compaction curves of control and fibre reinforced soils

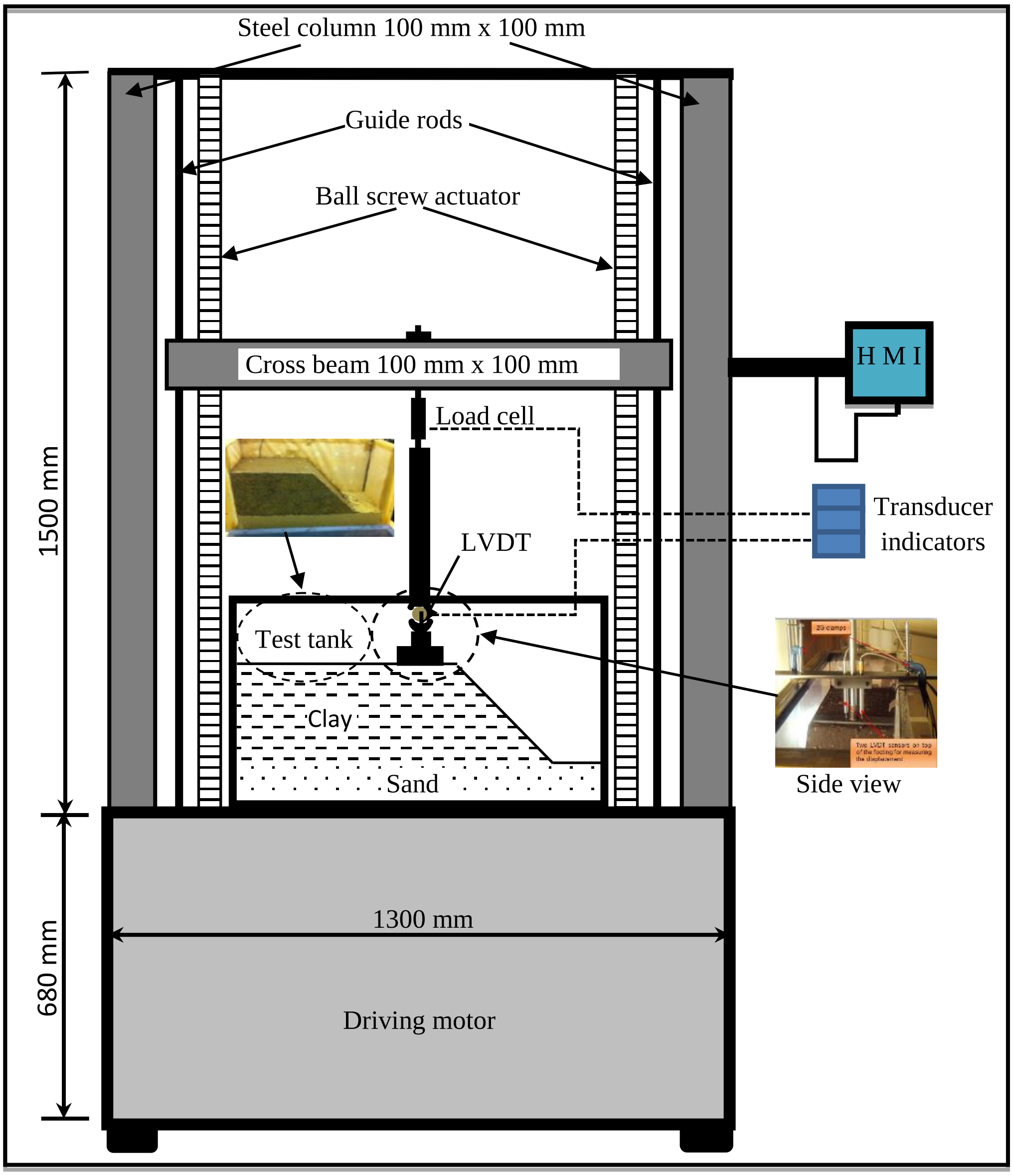


Fig. 2. Schematic drawing of the experimental set-up

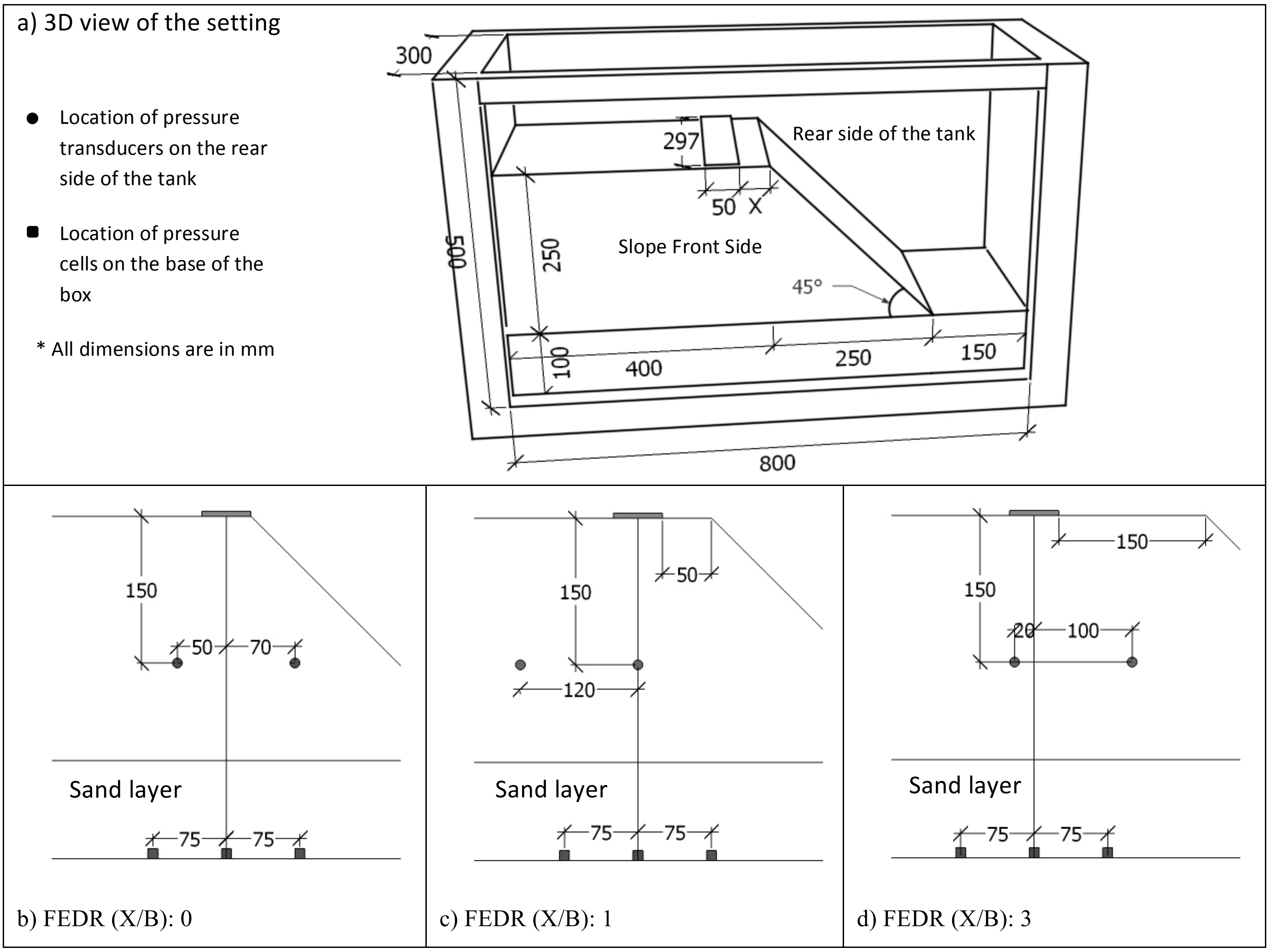


Fig. 3. Geometry of the model slope

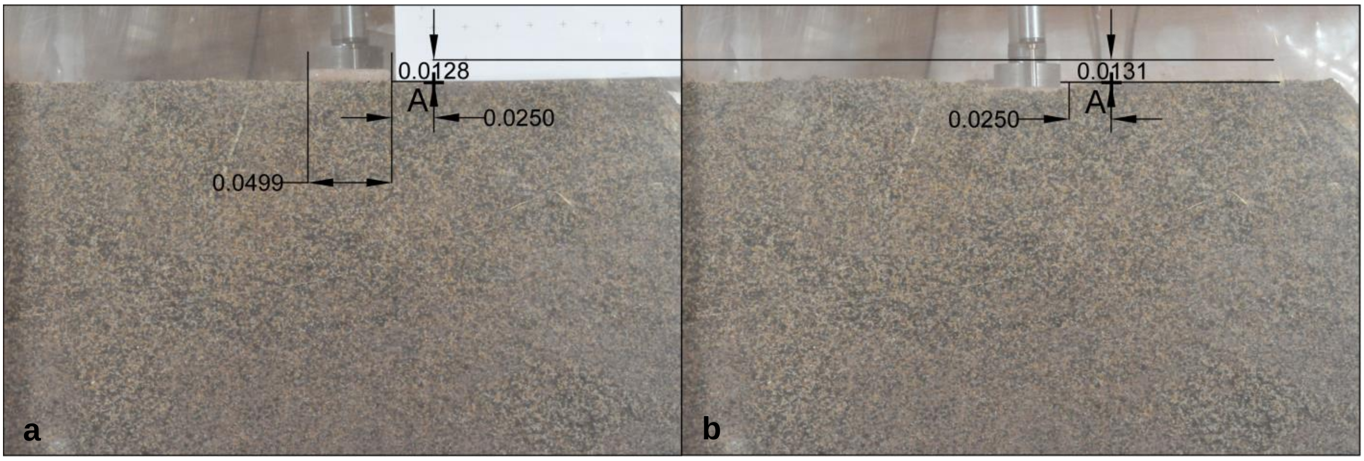


Fig. 4. Vertical distance (m) between point A and a known position
a) before loading b) after loading at 50 kPa footing pressure (FEDR = 3)

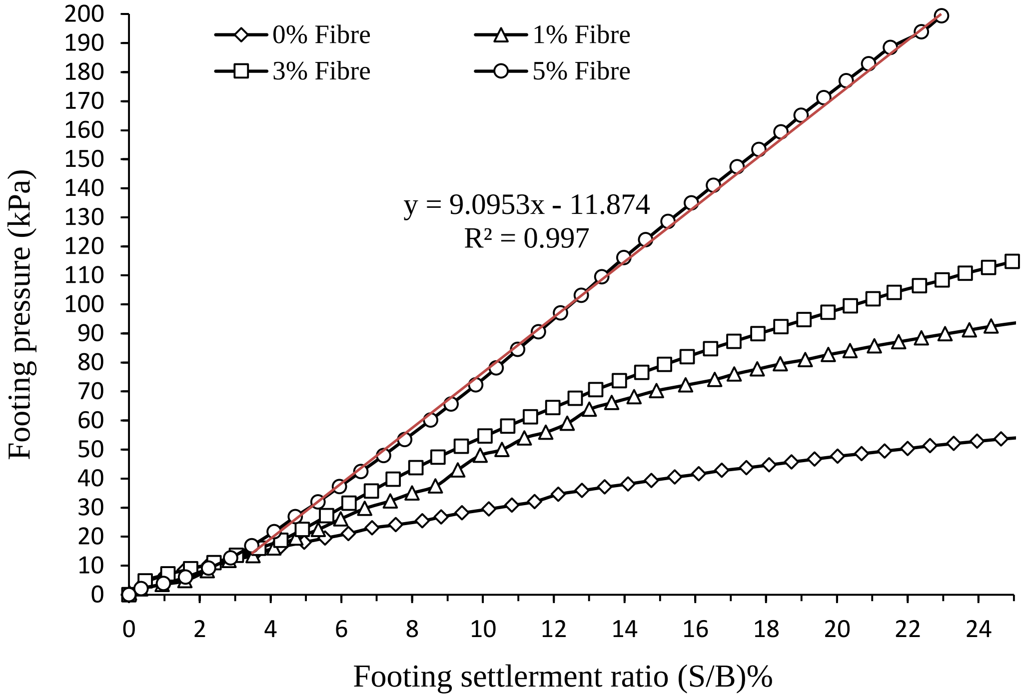


Fig. 5. Footing pressure curves versus footing settlement ratio (FEDR = 3)

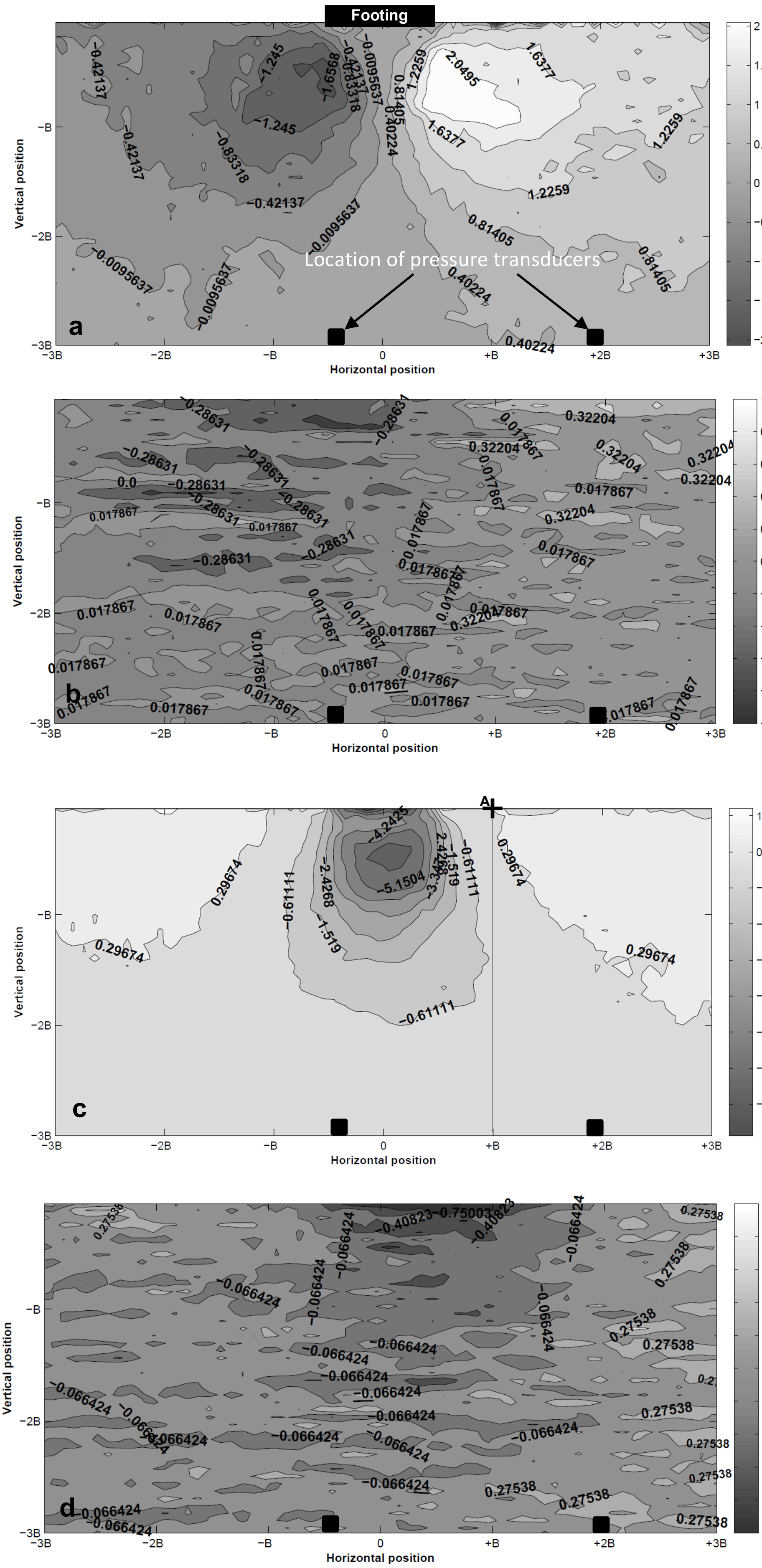


Fig. 6. Contours of horizontal (a & b) and vertical (c & d) displacement (mm) under footing pressure of 50 kPa for FEDR = 3: a,c) 0% fibre b,d) 5% fibre

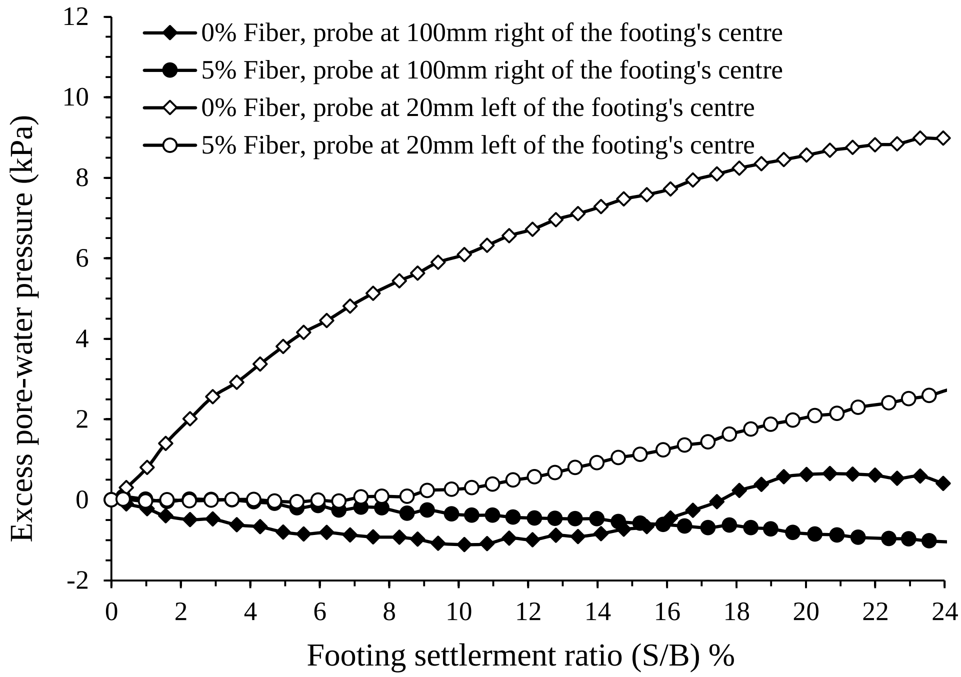


Fig. 7. Pore-water pressure curves versus footing settlement ratio (FEDR = 3)

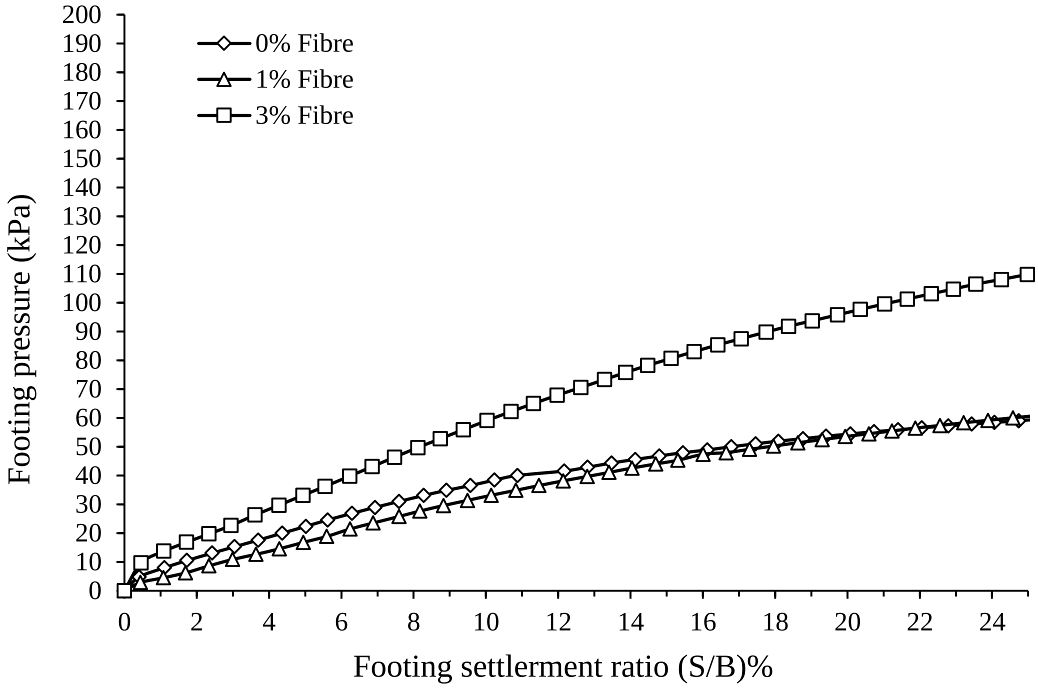

Fig. 8. Footing pressure curves versus footing settlement ratio (FEDR = 1)

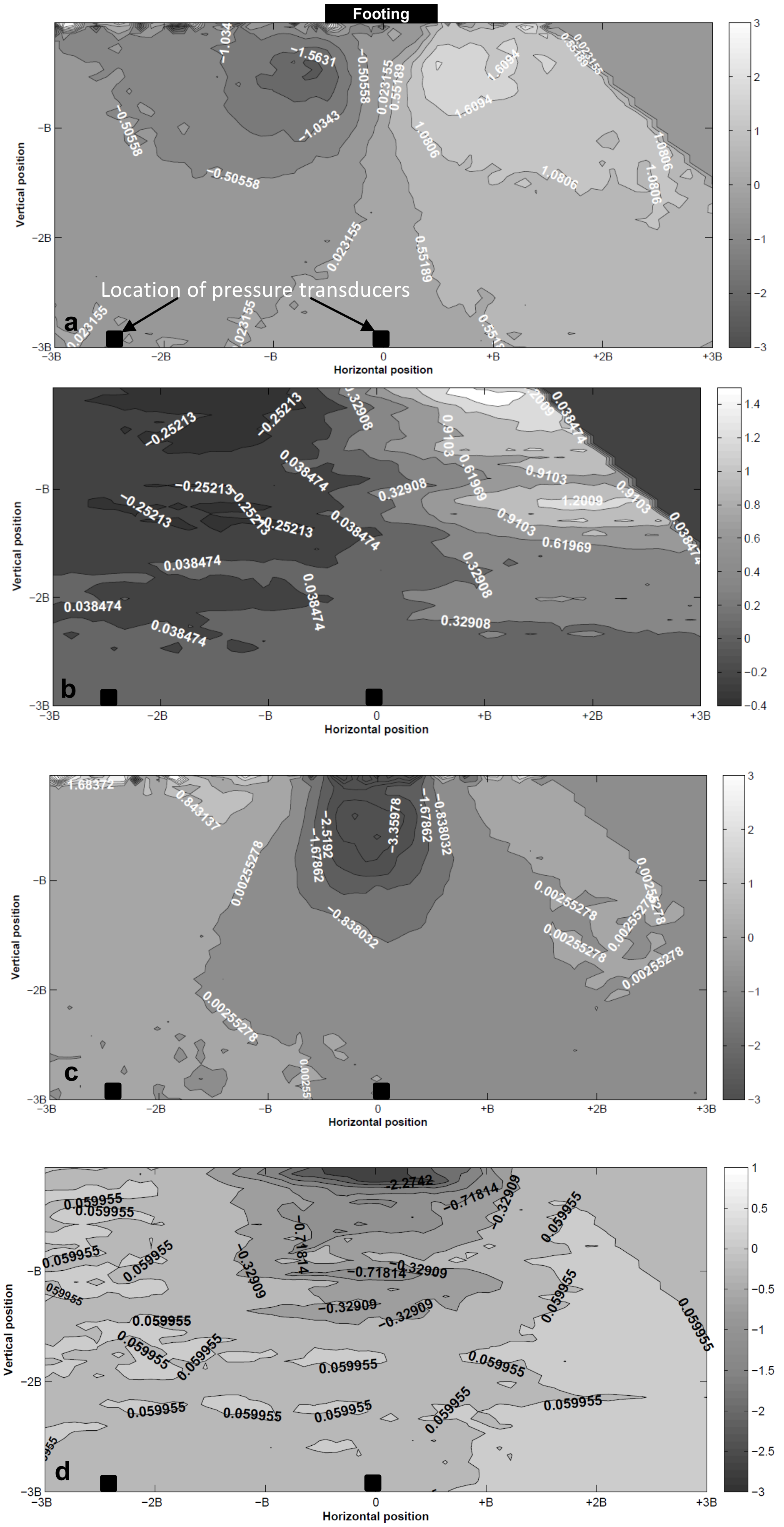


Fig. 9. Contours of horizontal (a & b) and vertical (c & d) displacement (mm) under footing pressure of 50 kPa for FEDR = 1: a,c) 0% fibre b,d) 3% fibre

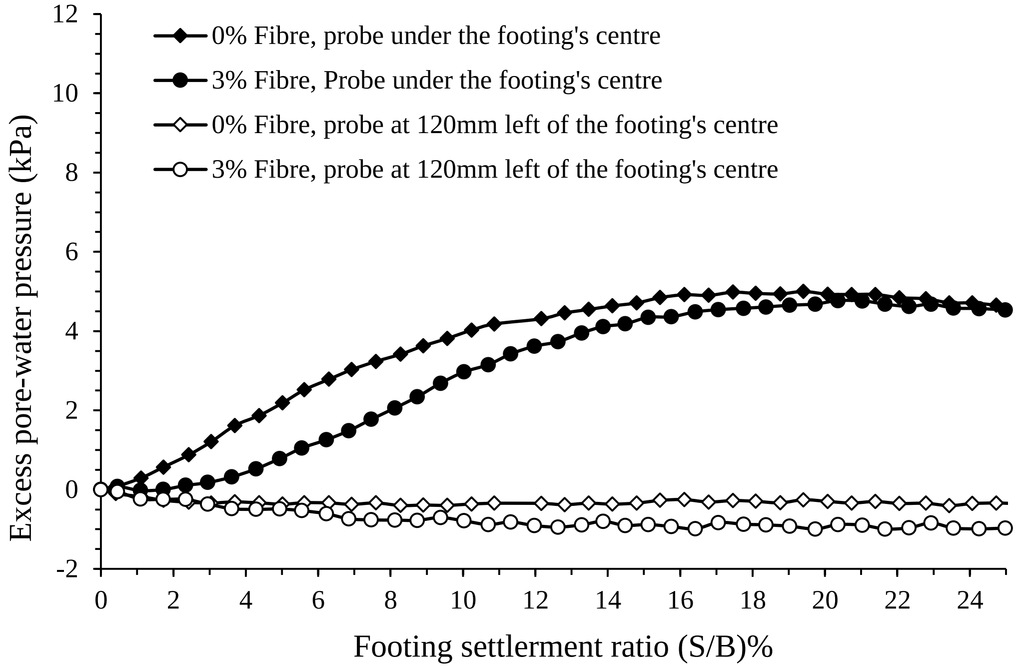


Fig. 10. Pore-water pressure curves versus footing settlement ratio (FEDR = 1)

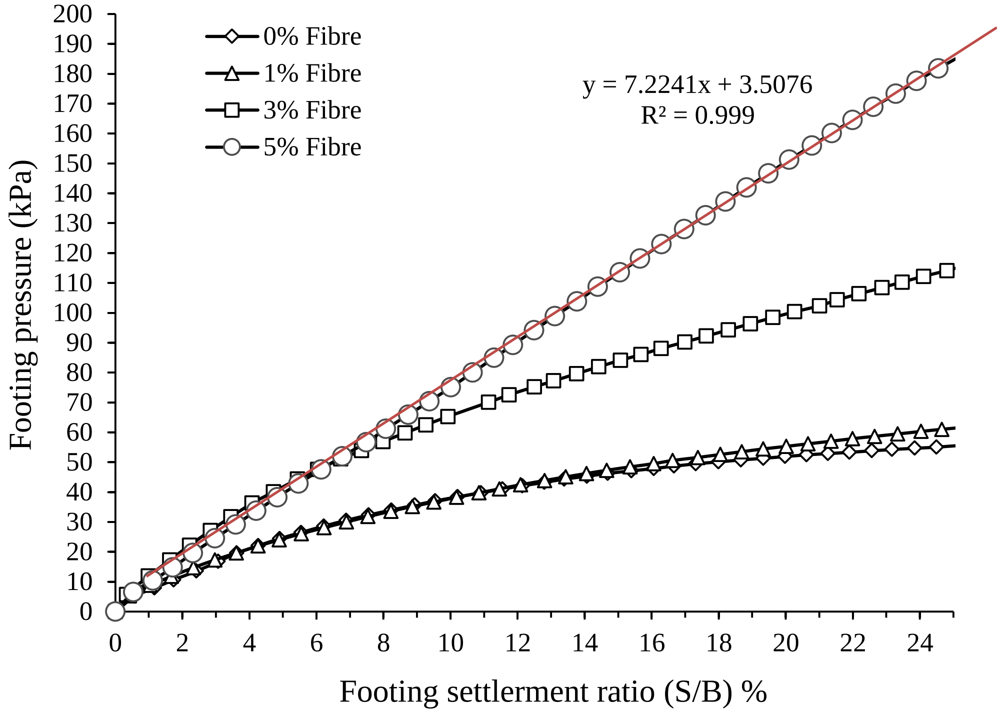

Fig. 11. Footing pressure curves versus footing displacement ratio (FEDR = 0)

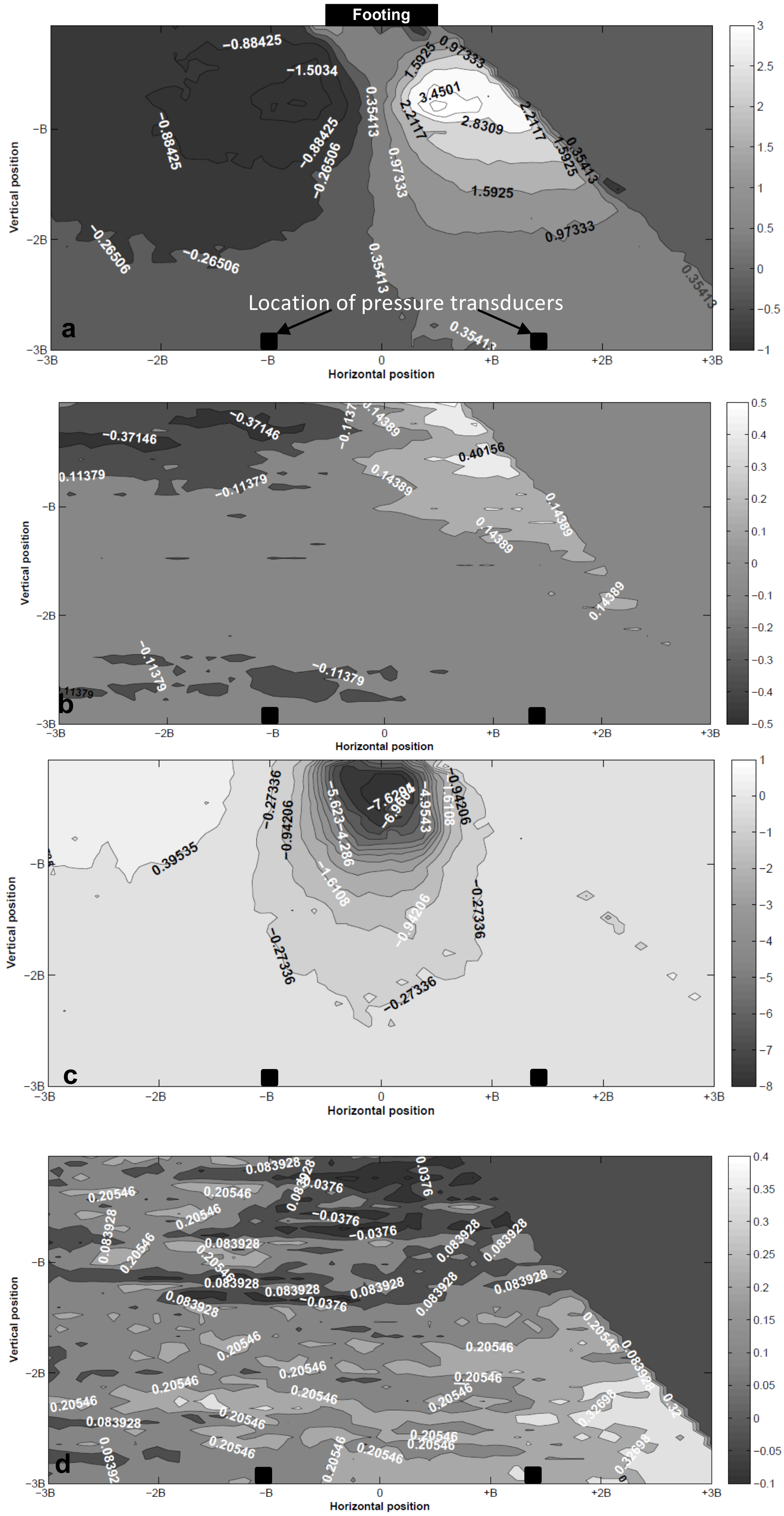

Fig. 12. Contours of horizontal (a & b) and vertical (c & d) displacement (mm) under footing pressure of 50 kPa for FEDR = 0: a,c) 0% fibre b,d) 5% fibre